EUROPEAN FUSION DEVELOPMENT AGREEMENT

EFDA–JET–CP(07)03/22

G. Arnoux, P. Andrew, M. Beurskens, S. Brezinsek, C. Challis, P. De Vries,
W. Fundamenski, E. Gauthier, C. Giroud, A. Huber, S. Jachmich,
X. Litaudon, R.A. Pitts, F. Rimini and JET EFDA contributors

Plasma-Wall Heat Loads in ITER-Like Advanced Tokamak Scenarios on JET

Plasma-Wall Heat Loads in ITER-Like Advanced Tokamak Scenarios on JET

G. Arnoux[1], P. Andrew[2], M. Beurskens[2], S. Brezinsek3, C. Challis[2], P. De Vries[2], W. Fundamenski[2], E. Gauthier[1], C. Giroud[2], A. Huber[3], S. Jachmich[4], X. Litaudon[1], R.A. Pitts[5], F. Rimini[1] and JET EFDA contributors*

[1] Association EURATOM-CEA, DSM/DRFC, CEA/Cadarache, F-13108 St Paul-Lez-Durance, France
[2] EURATOM/UKAEA Fusion Association, Culham Science Center, Abingdon, Oxon, OX14 3DB, UK
[3] Forschungzentrum Jülich GmbH, Institut f¨ur Plasmaphysik, Trilateral Euregio Cluster, EURATOM-Assoziation, D-52425 Jülich, Germany
[4] Association "EURATOM-Belgian State" Laboratory for Plasma Physics Koninklijke Militaire scholl - Ecole Royale Militaire Renaissancelaan 30 Avenue de la renaissance, B-1000 Brussels Belgium
[5] Association EURATOM-Confédération Suisse, Ecole Polytechnique Fédérale Lausanne (EPFL), CRPP, CH-1015 Lausanne, Switzerland
** See annex of M.L. Watkins et al, "Overview of JET Results ", (Proc. 21st IAEA Fusion Energy Conference, Chengdu, China (2006)).*

Preprint of Paper to be submitted for publication in Proceedings of the
34th EPS Conference on Plasma Physics,
(Warsaw, Poland 2nd - 6th July 2007)

INTRODUCTION

The Advanced Tokamak (AT) scenarios have been developed with the aim of long steadystate operation [1]. They operate at relatively low densities (central line average density: $n_{e,av} \leq 4 \cdot 10^{19}$ m^{-3} on JET) and high additional power (20MW $\leq P_{add} \leq$ 30MW on JET), necessary to ensure a large fraction of non inductive current. This leads to hot edge plasmas ($T_e \simeq$ 23/25eV at the inner/ outer target respectively on JET) and hence low recycling condition with partial divertor detachment difficult to achieve, if not impossible. The power handling capabilities of the Plasma Facing Components (PFC) during AT scenarios is a key issue [2] regarding the next JET enhancements: P_{add} = 45MW for 20s, and the ITER-like wall project: beryllium PFCs for the main chamber and a tungsten divertor [3]. For the first time on JET an attempt has been made to characterise the edge plasma of AT scenarios in ITER-like configuration. New AT scenarios have been developed to study their compatibility with the plasma-wall interaction. In particular impurity injection techniques have been developed for two reasons: the reduction of the continuous heat load on the divertor target by increasing the radiated fraction, which is discussed in the present paper, and the ELM mitigation by reducing the pedestal energy -compensated by the creation of an internal transport barrier (ITB)- which is discussed in [4]. Impurity injection techniques have also been studied on JET in hybrid scenarios with type-III ELMs [5].

The present paper is organised as follows: first the experiments and the heat load determination by infrared (IR) thermography are presented. The results of impurity injections experiments are then discussed, and conclusion drawn.

1. EXPERIMENTS AND RESULTS

The reference plasma discharge called ITER-AT is a high triangularity configuration (Figure 1a) with B_0 = 3.1T, I_p = 1.9MA, $q_{95} \simeq$ 5.0, δ = 0.42, and with 24MW additional power applied for 6s (144MJ total input energy). About 100MJ ($P_{rad}/P_{tot} \simeq$ 30%) is conducted to the PFCs 80% being conducted to the divertor (from thermocouple measurements) and at least 10% conducted to the upper dump plate (from the IR measurement). Figure 1b is an IR image of the JET in-vessel PFCs where the white areas denote the hottest elements. This illustrates that the main plasma-wall interaction is on the divertor and the upper dump plate. The bright spots on the outer wall are due to RF heating (ICRH) [6] rather than plasma-wall interaction. This is justified given that for these experiments the plasma-wall gap at the outer mid-plane is about 10cm when the scrape-off layer (SOL) e-folding length determined from the IR heat load profile (cf Figure 2f) is $\lambda_{SOL} \simeq$ 1.3cm. The present paper focuses its study on the divertor inner and outer target heat load measurement using the JET-EP wide angle IR camera [7].

The IR heat load profiles, $q_{IR}(s, t)$, s being the length along the surface of the poloidal cross-section of the tile (Figure 2e and 2f), are calculated from the temperature profiles (toroidal averaging of the target surface temperature, see example in Figure 1d) using the 2D non-linear code THEODOR [9]. The tiles are modelled with a rectangle cross-sections and the effect of the carbon layer on the

surface [10] is taken into account in the calculation assuming a uniform layer characterised by a heat transmission coefficient, asl (No heat capacitance) [11]. The heat flux through the layer is such that: $q = \alpha_{sl} \cdot (T_{surf} - T_{bulk})$, where T_{bulk} is the tile surface temperature and T_{surf} is the surface layer temperature seen by the IR camera. In the present configuration, tile 5 is a net erosion area (no layer): $\alpha_{sl,outer} = 200 kW/m^2K$ whereas the horizontal part of tile 1, where the peak heat load is measured (Figure 2e), is a deposition area: $\alpha_{sl,inner} = 5 kW/m^2K$.

Figure 2 illustrates two typical scenarios, one with and one without impurity injection. It shows that impurity injection reduces the outer target peak temperature (Figure 2c), thus the peak heat load (Figure 2d). The scenario has been repeated for different gas injection locations (GIM9 and GIM11, see Figure 1a), gas species (Neon (Ne) and Nitrogen (N_2)) and amount of gas. The total radiative power, P_{rad} (Figure 2b), is controlled using feed forward impurity injection (see wave form in Figure 2a). Despite a constant fraction of radiated power (ELMaveraged) during the discharge the L to H-mode transition is difficult to control and the ELM behaviour can change during the discharge ($20 \leq f_{elm} \leq 220 Hz$ [4]). For the divertor heat load study 200ms time windows are selected in both L and H mode phases in the [47;49] time interval in which the strike point positions are fixed. To compare the effect of different radiative fraction level, P_{rad}/P_{tot}, one determine the peak heat loads, $q_{av,inner}$ and $q_{av,outer}$, of the inner and outer targets respectively from the time averaged (200ms) profiles. As shown in Figure 2e and 2f the peak heat load coincides with the strike point position on tile 5 whereas on tile 1 the peak heat load is located on the horizontal part of the tile. The complex geometry of tile 1 combined with the strong variation of the pitch angle of the magnetic field lines along the tile make the interpretation of the heat load profile difficult. In the present work,“qav,inner, is taken at the maximum of the profile and not at the strike point position.

Figure 3 shows that qav,outer decreases by up to a factor 8 when $P_{rad}/P_{tot} \geq 50\%$ and this does not depend on the gas injection location or injected species whereas $q_{av,inner}$ is not significantly affected. In the ITER-AT configuration, the inner target heat load is difficult to decrease because the distance between the x-point and the target (about 10cm) is too short for the power to be dissipated by radiating process. In addition, the open divertor configuration leads to a low recycling regime. At high radiative fraction ($P_{rad}/P_{tot} \geq 50\%$) one find that qav,outer/qav,inner < 1 tough this number is to be taken cautiously. If the relative values of the heat load from tile to tile are reliable, the absolute value, hence the comparison between two tiles is more difficult because of the uncertainty due to the calculation. One find that on the tile 5 the accumulated energy calculated from the time and space integration of $q_{IR}(s, t)$, $E_{5,IR}$, is such that $E_{5,IR}/E_{5,TC} = 50-70\%$ where $E_{5,TC}$ is determined from the thermocouple measurements. This is not systematic and it is planned to investigate this discrepancy more in detailed in the future. On tile 1 the discrepancy is rather $E_{1,IR}/E_{1,TC} = 75-90\%$. However the shape of tile 1 cross-section suggests that a rectangle cross-section model is probably not appropriate.

CONCLUSION

The present work provides the first characterisation of the divertor heat load using IR thermography during advanced tokamak scenarios in ITER-like cofiguration on JET. In future operation (power upgrade, ITER-like wall), divertor heat load might be challenging
on the inner target, whereas on the outer target it can be significantly reduced using Neon or Nitrogen injection techniques. The gas species and gas injection location are not determinant parameters for the heat load reduction.

REFERENCES

[1]. A.A. Tuccillo et. al. Nucl. Fusion, **46**, 2006.

[2]. X. Litaudon and et. al. Proc. in this conference, 2007.

[3]. J. Pamela and et. al. J. Nucl. Mater., **363-365**:1–11, 2006.

[4]. M. Beurskens and et. al. Proc. in this conference, 2007.

[5]. Y. Corre and et. al. Proc. in this conference, 2007.

[6]. L. Colas and et. al. Proc. in this conference, 2007.

[7]. E. Gauthier and et. al. Proc. in 24th Symposium on Fusion Technology, Warsaw, Poland, 2006.

[8]. S. Jachmich and et. al. Proc. in this conference, 2007.

[9]. A. Herrmann and et. al. Plasma Phys.Control. Fusion, **37**:17–29, 1995.

[10]. P. Andrew and et. al. J. Nucl. Mater., **313-316**:135–139, 2003.

[11]. T. Eich and et. al. Plasma Phys. Control. Fusion, **49**:573–604, 2007.

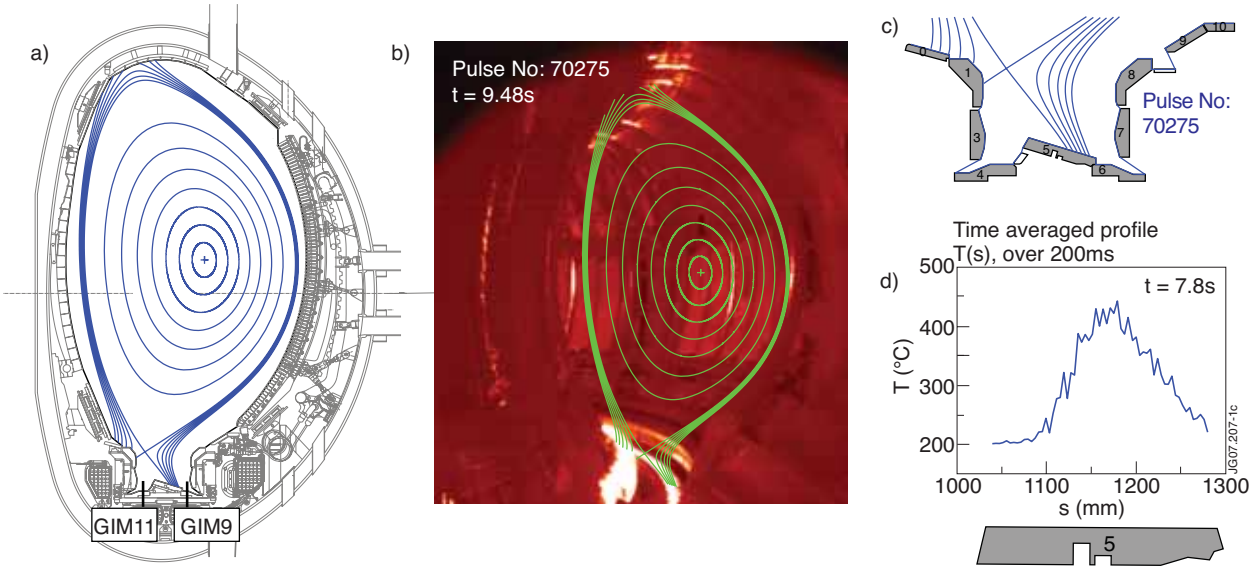

Figure 1: (a) Schematic view of the JET cross-section and the ITER-AT configuration (constant magnetic flux surfaces calculated with EFIT). Two gas injection locations, in the divertor SOL and in the private flux region are labelled GIM9 and GIM11 respectively. (b) Infrared image taken with the JET-EP wide angle IR camera (KL7) with superimposed flux surfaces (pulse number=70275). (c) Cross-section of the JET divertor with numbered tiles. The spacing of the SOL magnetic flux surfaces corresponds to 5mm at the radius at outer mid-plane. (d) Example of an IR temperature profile on the outer target after toroidal averaging at t = 7.8s

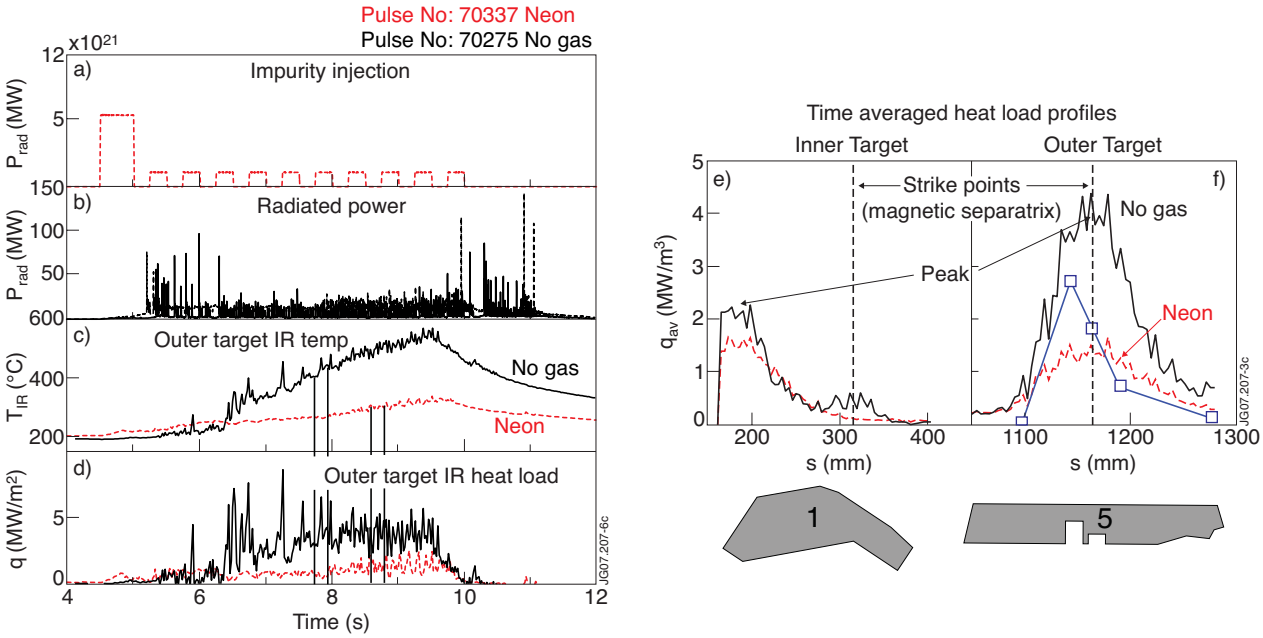

Figure 2: Two typical discharges without (70275) and with (70337) impurity injections. (a) Impurity injection wave form. (b) Total radiated power. (c) Outer target IR peak surface temperature. (d) Outer target IR peak heat load. (e) and (f) Time averaged IR heat load profiles for inner and outer target respectively. The outer target profile is compared with the heat load determined from the Langmuir probe measurements (squares) [8].

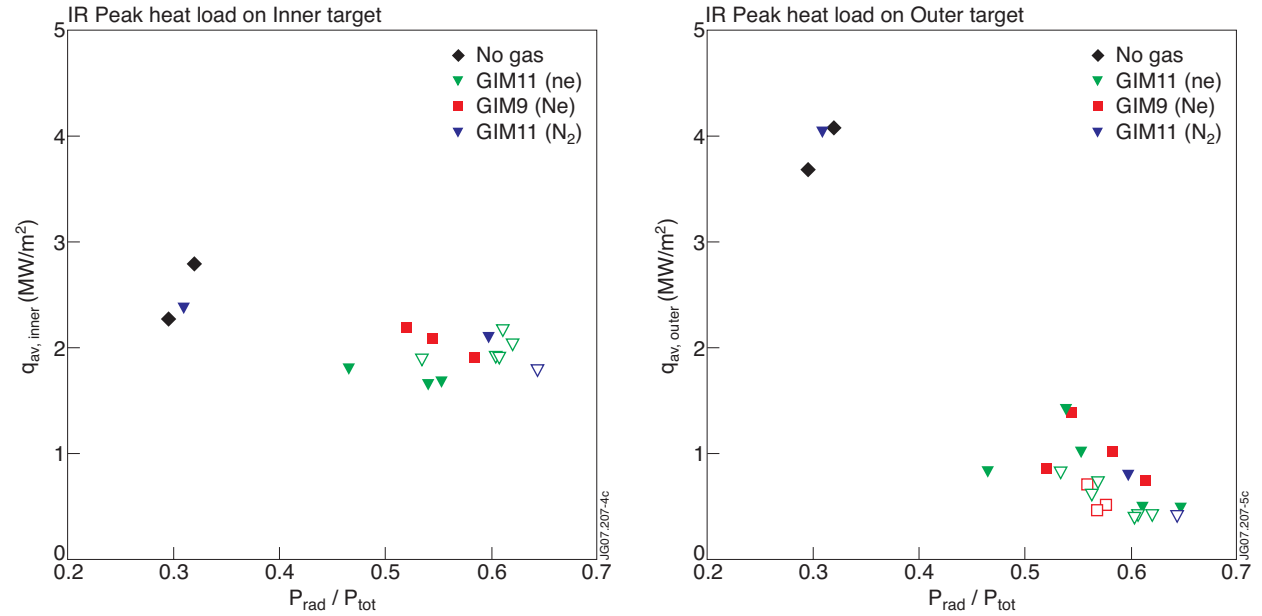

Figure 3: Peak heat load as a function of the fraction of radiated power (a) on the inner and (b) on the outer target calculated from IR thermography. The impurities ares injected in the private flux region (triangles) or in the SOL (squares) and leads to either H-mode (solid symbols) or L-mode (open symbol). Diamonds indicate the reference pulses with no impurity injection.